Geophysical Research Letters

RESEARCH LETTER
10.1029/2023GL103812

Mega Forest Fires Intensify Flood Magnitudes in Southeast Australia

Zhenwu Xu[1,2], Yongqiang Zhang[1], Günter Blöschl[3], and Shilong Piao[4]

[1]Key Laboratory of Water Cycle and Related Land Surface Processes, Institute of Geographic Sciences and Natural Resources Research, Chinese Academy of Sciences, Beijing, China, [2]University of Chinese Academy of Sciences, Beijing, China, [3]Institute of Hydraulic and Water Resources Engineering, Technische Universität Wien, Vienna, Austria, [4]State Key Laboratory of Tibetan Plateau Earth System, Resources and Environment, Institute of Tibetan Plateau Research, Chinese Academy of Sciences, Beijing, China

Key Points:

- The unprecedented 2019–2020 forest fires intensified subsequent river flood magnitudes in southeast Australia
- Forest fire amplification of floods is divergent in different regions
- Regional divergence in fire impacts is attributed to different burned areas and dominant flood generating mechanisms

Supporting Information:

Supporting Information may be found in the online version of this article.

Correspondence to:

Y. Zhang,
zhangyq@igsnrr.ac.cn

Citation:

Xu, Z., Zhang, Y., Blöschl, G., & Piao, S. (2023). Mega forest fires intensify flood magnitudes in southeast Australia. *Geophysical Research Letters*, *50*, e2023GL103812. https://doi.org/10.1029/2023GL103812

Received 22 MAR 2023
Accepted 7 JUN 2023

© 2023. The Authors.
This is an open access article under the terms of the Creative Commons Attribution License, which permits use, distribution and reproduction in any medium, provided the original work is properly cited.

Abstract Recent forest fires potentially intensify flood hazards. However, forest fire amplification of floods is not well understood at a large scale due to the complex compound impacts of forest fires and climate variability, while available small-scale cases may not represent regional changes. Here, we show that the 2019–2020 mega forest fires in southeast Australia, with unprecedented burned areas, significantly ($p < 0.05$) increased the peak discharges of floods during the 2 years after the fires. Spatially, fire impacts on these floods are much stronger in regions with winter-dominated and uniform rainfall but insignificant in regions with summer-dominated rainfall. The regional divergence reveals that burned areas can aggravate floods by exacerbating infiltration-excess runoff processes but may not exert significant effects where saturation-excess processes dominate. People may be increasingly exposed to such flood hazards, especially in regions where forest fires have become more frequent under climate change.

Plain Language Summary Wildfires and floods are both natural hazards that cause damage to lives and properties. Understanding how these two are linked is critical not only for catchment hydrological processes but also for hazard control and water resources management. However, it is unclear whether mega forest fires can influence the subsequent floods on a large scale. This study demonstrates that the recent mega forest fires in southeast Australia have significantly amplified floods for most fire-impacted catchments. Apart from raising awareness of global fire activities, this study indicates that people living in the fire-prone area may be also susceptible to more flood hazards after fires in the future.

1. Introduction

Wildfires are uncontrolled fires that usually occur during severe droughts and/or heatwaves. In contrast to controlled, prescribed fires, wildfires can directly cause billions of dollars in damage to properties and ecosystems, and indirectly affect the carbon cycle and climate (Godfree et al., 2021; Loehman, 2020; Moritz et al., 2014). With changes in vegetation and soils, wildfires can also affect hydrological processes. Over short periods of time, they may reduce forest water use by the large loss of vegetation cover (Collar et al., 2021), and they may reduce infiltration by soil hydrophobicity after fires (Ebel & Moody, 2017). Both processes may cause changes in catchment water yields, impacting the regional water supply (Hallema et al., 2018; Khaledi et al., 2022; Paul et al., 2022; Wine et al., 2018; Xu et al., 2022). Due to profound influences on the environment and society, increasing fire events have recently attracted great public concern, especially for flammable forests in populated temperate zones (Bowman et al., 2020).

In burned forests, intense rainfall can produce large runoff, possibly amplifying flood magnitudes. Research into small-scale measurements and experiments at burned hillslopes have advanced our understanding of how changes in vegetation and soils, especially the soil water repellency effect on infiltration (Larsen et al., 2009; Letey, 2001; Moody & Ebel, 2012), may trigger large surface runoff under heavy rainfall. However, forest fire effects on the physical properties such as soil hydraulic properties are transient in time and variable in space (Ebel, 2022). Due to the complex interaction between burned landscapes and variable mesoscale precipitation (Kean et al., 2011; Liu et al., 2022), post-fire hydrologic responses can range from no response to catastrophic floods and deadly debris flows in diverse locations throughout the world (Lane et al., 2006; Moody et al., 2013; Noske et al., 2022).

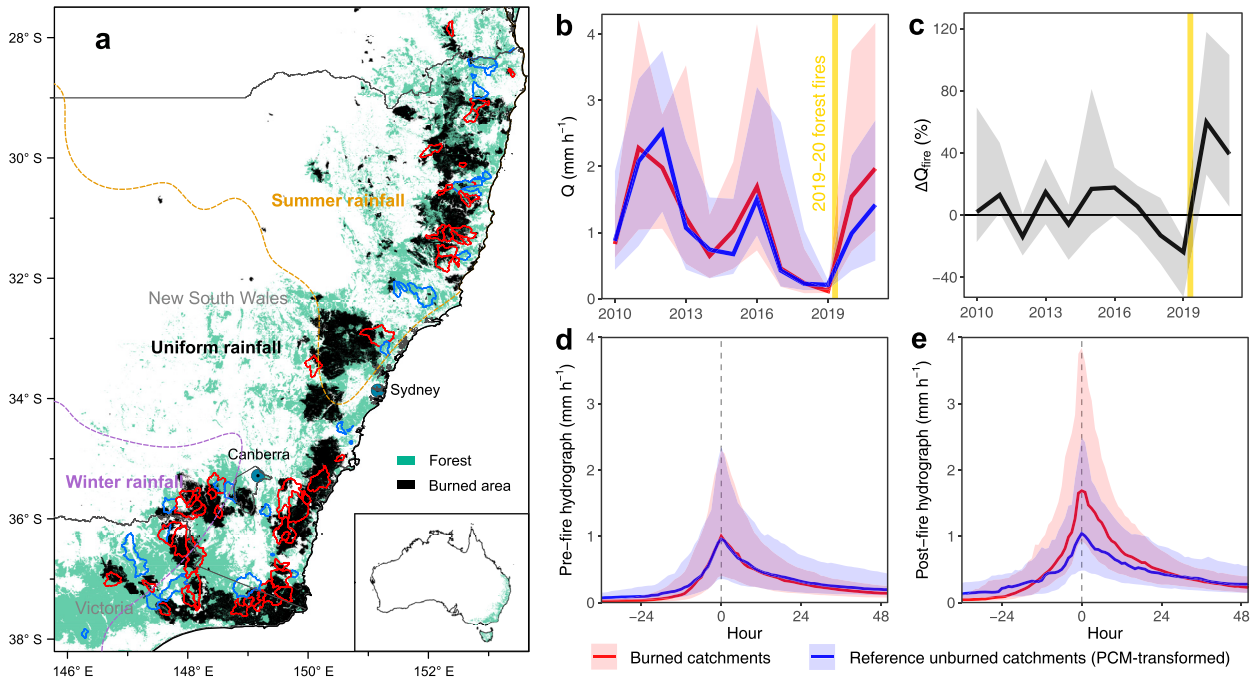

Figure 1. Intensified flood magnitudes after the 2019–2020 mega forest fires in Australia. (a) Unprecedented burned areas of the 2019–2020 forest fires and paired catchments used in the analysis. Australia's temperate broadleaf and mixed forests are shown in green, and the BA of the 2019–2020 forest fires are shown in black. The red and blue polygons are the burned and unburned catchments, respectively. (b) The pre-fire similarity and the post-fire disparity in the interannual variations in the annual maximum flood peak discharge (Q) of paired catchments. (c) Estimated fire effects on flood peaks (ΔQ_{fire}) in burned catchments. (d and e) Pre-fire similarity and post-fire disparity in flood hydrographs of paired catchments. Solid lines and shaded bands in panels (b–e) are the spatial medians and the 30% and 70% ranges. The median hydrographs in panels (d and e) are medians across catchments and all years for the two periods, while hour 0 is the time of peak discharge.

As these small-scale cases were taken in different times and spaces and often limited to hillslopes and several small basins, the large-scale impacts of forest fires on river floods remain poorly understood.

Generalizing regional fire effects on flood magnitudes is crucial for understanding how these natural hazards may cascade under climate change and variability. The El Niño-Southern Oscillation (ENSO) can cause interannual variations in precipitation (and thus moisture conditions) in certain regions of the world, resulting in droughts, wildfires, and floods (Abram et al., 2021; King et al., 2020; Van Dijk et al., 2013; Ward et al., 2014). The frequency of ENSO extremes (El Niño and La Niña) has increased under greenhouse warming (Cai et al., 2014, 2015). As a consequence of precipitation redistribution, one natural hazard may cascade to another within one or more years (Chen et al., 2017; Kemter et al., 2021). Thus, the coincidence of large forest fires and the subsequent floods in some fire-prone areas is challenging the common view that floods are water extremes mostly related to heavy rainfall or snow melting. Therefore, elucidating whether regional-wide forest fires can intensify river floods is informative for future warning and management of cascading natural hazards.

The recent 2019–2020 mega forest fires in southeast Australia provide a unique "natural experiment" for understanding the impact of large-scale fires on floods. "Megafire" is commonly used for defining a large fire that burns over a certain limit of land, typically 100,000 ha (Collins et al., 2021). Compared with other megafires, the 2019–2020 mega forest fires in southeast Australia are unique as 21% of temperate broadleaf and mixed forests were burned during the fire season, unprecedented in the historical record, while the annually burned area (BA) is typically below 2% (Figure 1a) (Boer et al., 2020). The megafires occurred during a historically anomalous drought (Bowman et al., 2021) that was preconditioned by rare 2-year consecutive concurrences of positive Indian Ocean Dipole and El Niño conditions (Wang & Cai, 2020). In the ensuing 2 years, 2020–2021, eastern Australia experienced heavy floods as La Niña brought much more rainfall. Apart from the wet period, the mega forest fires may have caused amplified peak flows across large geographic regions during the same period, as rivers associate burned forests and unburned landscapes.

This study aims to examine if mega forest fires, with large burned areas (some are even unprecedented), can intensify flood magnitudes at a large scale. As climate variability and forest fires can exert overlapping influences

on post-fire floods, the paired catchment method (PCM) was used for determining the impact of 2019–2020 forest fires in southeast Australia. After a methodical filtering process, we identified 57 forested catchments burned by the forest fires and their unburned reference catchments. Based on a good similarity of transformed flood peak discharges during the pre-fire period (2010–2019), we attribute the differences in peak discharges between paired catchments to the impact of forest fires during the post-fire period (2020–2021). With this huge natural experiment, this study provides observational evidence of the intensifying impact of mega forest fires on flood magnitudes and discusses their causes.

2. Materials and Methods

2.1. Data and Catchments

The streamflow data were obtained from the Australian Bureau of Meteorology (BOM). For hourly analysis of floods, almost all flood series data (96.5%) were standardized and aggregated from data with sub-hourly resolution (mostly 15 min), which are widely available for the study period 2010–2021. For a small part of the flood series, data were linearly interpolated only when the missing gap was less than 4 hr. For the daily analysis of floods, all flood series data were standardized and aggregated as daily mean values without gap-filling. We used Eckhardt's digital filter (Eckhardt, 2005) to separate base flow and quick flow. The two parameters, that is, recession constant and maximum base flow index, were automatically determined by an automatic base flow identification technique (Cheng et al., 2016) and a backward filtering operation (Collischonn & Fan, 2013), respectively. As BOM does not provide boundaries for these catchments, they were delineated by an automatic outlet relocation algorithm (Xie et al., 2022) with the flow direction data from MERIT hydro (Yamazaki et al., 2019). Catchment daily rainfall data were obtained from the SILO gridded data, which are interpolated from site observations and have a high accuracy in this data-rich region (Jeffrey et al., 2001). The hourly rainfall data were obtained from the spatially nearest rainfall gauge for each catchment.

Burned area data during 2010–2021 were obtained from the different state agencies of Australia, including Victoria, New South Wales, and Queensland (Canadell et al., 2021). Specifically for the 2019–2020 forest fires, BA data were derived from the more accurate fire severity data, which is validated against observations and has better accuracy than other products (Collins et al., 2018). Here, BA is defined as an area that experienced low, moderate, high (and extreme) severity of fires (Bowman et al., 2021). However, as these data did not give the exact timing of forest fires for each catchment, they were instead obtained from Moderate-resolution Imaging Spectroradiometer (MODIS) Collection (C) 6 MCD64A1 BA data (Giglio et al., 2018). As an important indication of vegetation change, leaf area index (LAI) data were obtained from MODIS C6 MOD15A2H LAI data (Myneni et al., 2015).

To select suitable unregulated catchments for the analysis of flood changes, the catchments were filtered based on the following criteria (Figure S1 in Supporting Information S1): (a) no large dam or reservoir is located in the catchments; (b) agricultural land use is less than 5%; (c) coverage of forest ecosystem is larger than 50%; and (d) the catchment area is less than 1,500 km^2. Furthermore, qualified annual streamflow data (>95% coverage) should be available for more than 7 years during the pre-fire 2010–2019 and for both years during the post-fire 2020–2021. Near the 2019–2020 forest fires, the catchments are mainly located in New South Wales and eastern Victoria. According to BA data from state agencies, unburned catchments were not impacted by major fire activity during both pre-fire period and post-fire period (annual BA <20%). Burned catchments were impacted by fire activity during the 2019–2020 forest fire season with annual BA ≥20% (Hallema et al., 2018; Williams et al., 2022) but not impacted by other fires. Finally, 155 catchments were obtained, including 63 burned catchments and 92 unburned catchments.

Rainfall seasonality is an important kind of climate classification for regional flood studies. According to BOM, the selected catchments locate in different seasonal rainfall zones, including the summer, uniform, and winter rainfall zones. These zones were determined by the median annual rainfall (based on the 100-year period from 1900 to 1999) and seasonal incidence (the ratio of the median rainfall over the period November–April to the period May–October) with different thresholds. Here, the gridded seasonal rainfall zone data from the BOM were smoothed as a vector image by the R package smoothr, which keeps the basic spatial pattern of seasonal rainfall.

2.2. Flood Events and Flood Generating Conditions

Annual maximum floods (AMF) were selected as the definition of floods in this study, which can show the inter-annual variability of flood magnitudes. Before obtaining AMF, independent rainfall-runoff (RR) events

were first identified. The maxima in the time series of streamflow are possible peaks of RR events. For independence, the starting point of an RR event was considered the first point of quick flow occurrence before the peak discharge (total flow), while the end point was taken as the first point of quick flow termination after the peak discharge. Meanwhile, the total flow at the start point and the end point of the RR event should be larger than 10% of the peak discharge. Otherwise, the point of the 10% limit was set for obtaining the start point and the end point. This avoids the possible inaccurate base flow separation that causes persistent low base flow and leads to an overestimation of flood duration. In hourly streamflow data, a new event was included if all of the following conditions were met: (a) direct flow occurs, (b) peak flow is higher than a peak threshold (Sikorska et al., 2015) (here, long-term average flow), (c) the streamflow data do not overlap with that of larger RR events in the previous extraction step, and (d) the event duration is longer than an assumed threshold (here, 6 hr to account for flash floods in the region). Specifically, the minimum event duration is 2 days for daily data. In descending order of streamflow maxima, we identified independent RR events based on the above criteria and subsequently AMF.

Flood generating conditions, including rainfall and soil moisture characteristics, were also obtained for each flood event. Rainfall conditions contributing to floods are represented by rainfall volume and rainfall duration, which were obtained from the hourly rainfall data. While accounting for the effective rainfall that contributes to the flood event, a window is set between the 12 hr prior to the start point of flood rising limb and the time of the end point of flood falling limb. To avoid counting intermittent rainfall, the rainfall duration that contributes to the flood is defined as the minimum duration that covers 80% of the total rainfall volume. In addition, soil moisture condition was extracted from the daily output of the Australian Water Resources Assessment Landscape model (AWRA-L) (Frost & Shokri, 2021), which has been extensively evaluated against in situ soil moisture observations with correlations similar to, or exceeding, those of remotely sensed products (Holgate et al., 2016). Here, soil moisture from the upper 1 m of the soil profile was used, which is found to be most correlated with flood response (Wasko et al., 2020).

2.3. Paired Catchment Method

The PCM is often recognized as the most simple but robust method for detecting the effects of disturbances on catchment-scale hydrology (Bren & Lane, 2014; Brown et al., 2005; Xu et al., 2022). Assuming that in two paired catchments, similar in climate, vegetation cover, and catchment properties, the correlation between their streamflow will remain the same if their vegetation cover remains the same. Here, we extend this classical method for flood analysis, which assumes that if no disturbances from forest fires occur, the AMF in a catchment has a similar process as that in another catchment. In practice, the AMF events of a burned catchment were paired with the nearby RR events with the maximum peak discharge of the reference unburned catchment. To ensure similarity, the gap between a burned AMF and the unburned maximum RR event was taken as less than 5 days. In this study, the mean difference in timings of paired events is only 0.8 days, supporting a similar RR process.

Specifically, assuming that in two catchments with similar climates and forest cover, the flood processes are similar without fire disturbance. Before forest fires, the relations between their flood peak discharges can be described by a linear regression model in log space.

$$\log(Q_b) = \log(Q_{\text{ref}}) + \varepsilon = \alpha \log(Q_c) + \beta + \varepsilon \tag{1}$$

where Q_b and Q_c are the observed flood peak discharges of the burned catchment (b) and the reference/unburned control catchment (c). Q_{ref} is the modeled value of Q_b without fire effects. α and β are the coefficient and the y-intercept, respectively. ε is the residual of the model.

After forest fires, this pairing relationship can be used for modeling the Q_{ref} unimpacted by fires. Therefore, fire impact on flood magnitudes can be extracted by an observation-modeling scheme (observed impacted vs. modeled unimpacted) (ΔQ_{fire}, %):

$$\Delta Q_{\text{fire}} \approx (Q_b - Q_{\text{ref}})/Q_{\text{ref}} \tag{2}$$

In PCM, the pairing relationship between each burned catchment and their best reference unburned catchment has the lowest root mean squared error among all possible unburned catchments. Meanwhile, using the same α and β in Equation 1, flood hydrographs of the unburned catchment can also be transformed as the references. Paired catchments with poor performance ($R^2 < 0.4$) are excluded from the analysis (Figure S1 in Supporting Information S1).

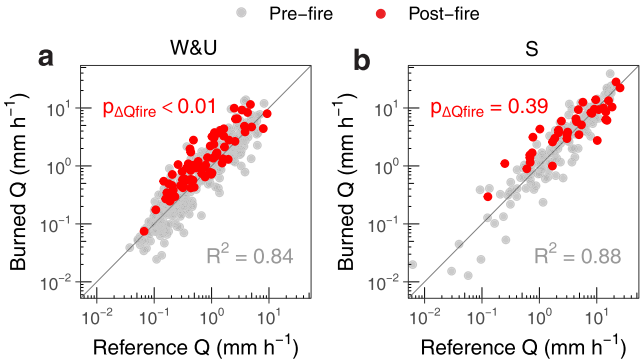

Figure 2. Divergent regional forest fire impacts on flood peak discharges. (a) Significant increases in flood peak discharges (Q) after forest fires in winter-dominated and uniform (W&U) rainfall catchments, indicated by the p value of the differences between burned flood peak series and the reference unburned series ($p_{\Delta Qfire}$); (b) Similar plot but insignificant changes in Q after fires for summer (S) rainfall-dominated catchments. The overall accuracy of the paired catchment methods is indicated by the R^2 for the pre-fire period.

In this study, floods during the pre-fire period 2010–2019 and the post-fire period 2020–2021 strictly occurred before and after the forest fires, respectively (Figure S2 in Supporting Information S1). For the hourly flood series, 57 of the 63 burned catchments (Figure 1a) yield satisfactory results in the PCM (R^2 = 0.41–0.99, median 0.78). The PCM using daily flood series data also shows good paring results, with a median R^2 of 0.81 for also 57 catchments. With no initial overall bias after linear transformation, a high agreement in pre-fire pairing (Figures 1b and 1d) indicates that the method is reliable for estimating forest fire effects on flood magnitudes, especially in an ensemble way (overall R^2 being 0.86 for flood peaks pairing).

2.4. Test of Significance

To test whether forest fires have significantly aggravated floods in these burned catchments, we conducted Student's t-test to evaluate the differences between the burned Q_b and the reference unburned Q_{ref} (Table S1 in Supporting Information S1). The flood peak discharges were log-transformed to remove the positive skewness and suit the t-test. Two significance levels at 0.05 and 0.01 were set for the difference test.

3. Results

3.1. Mega Forest Fire Intensify Flood Magnitudes

Taking the 57 burned catchments as an ensemble (Figure 1a), the forest fires significantly ($p < 0.05$) increased the hourly flood peak discharges by a median of 49% during 2020–2021. Fire impacts on flood magnitudes, defined as relative changes in flood peak discharges in comparison with those of reference unburned states, are overall stronger during the first year (on median 60%) than those during the second year (39%) after fires (Figure 1c). Comparison of the shapes of flood hydrographs provides more intuitive intensifying impacts of forest fires on floods (Figures 1d and 1e). To further test the robustness of our findings, we conduct a similar data-based analysis but on a daily scale. This analysis also suggests that the forest fires increased ($p < 0.10$) flood peak discharges by a median of 35% (Figures S3 and S4 in Supporting Information S1). The magnitude of the changes in hourly flood peak discharges is larger than that of the daily results, indicating that the forest fires caused a greater likelihood of hazard of instantaneous flood damages. In general, the present paired catchment results suggest that mega forest fires have intensified subsequent flood magnitudes in southeast Australia.

3.2. Regional Divergence

Spatially, forest fire impacts on flood magnitudes are regionally divergent. In those flood events, they are much stronger and significant ($p < 0.01$) in the catchments with winter-dominated or uniform rainfall located south of New South Wales and eastern Victoria (Figure 1a), where the median flood peak increased by 67% (Figure 2a). In contrast, the regional fire impacts are not significant ($p = 0.39$) in the summer rainfall-dominated catchments (Figure 2b). The daily data also show a similar regional divergence (Figures S4e and S4f in Supporting Information S1). To test if such regional divergence of burned catchments belongs to the bias of the paired catchment design, we conducted a similar analysis but for every single unburned catchment by selecting the best match from all other unburned catchments. As these unburned catchments have a low portion of BA, the insignificant differences between observation and prediction indicate that the overall bias is low ($p > 0.05$, Figure S5 in Supporting Information S1), supporting the existence of divergent regional fire impacts.

3.3. Causality Analysis

The insignificant fire impacts in summer rainfall-dominated catchments may be associated with the overall lower burned areas, and wetter flood generating conditions of those flood events (Figure 3). In specific, these catchments not only have smaller declines in LAI (determined by a similar PCM), but also experienced more rainfall and had higher soil moisture both prior to and during floods (Figure 3). As a cause, fire impacts can

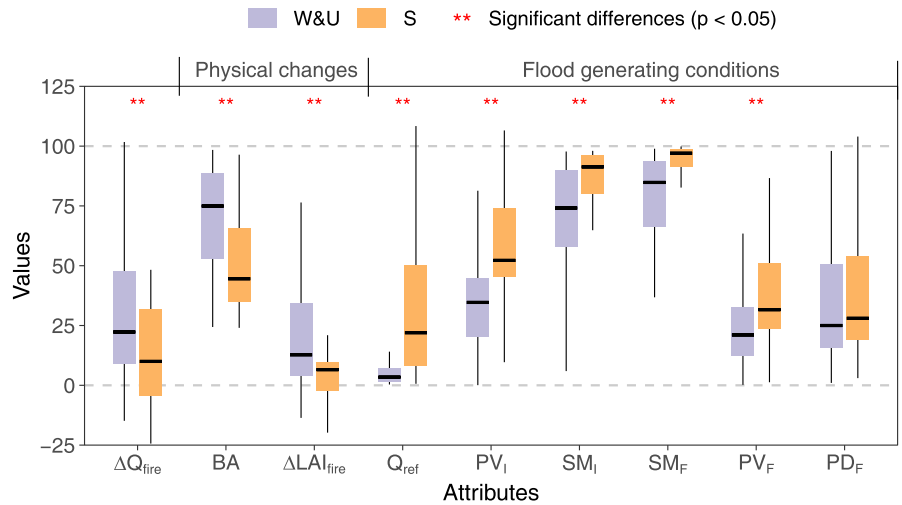

Figure 3. Divergent regional forest fire impacts on flood magnitudes are aligned with different burned areas and flood generating conditions. To make attributes at similar values, scaling factors are applied to some attributes. Between winter-dominated and uniform (W&U) rainfall catchments and summer (S)-dominated rainfall catchments, fire impacts on peak discharges (ΔQ_{fire}, unit of % multiplied by 1/3) can be linked with catchment burned area (%), the fire-induced leaf area index declines at the month of the flood event (ΔLAI_{fire}, %), and the reference peak discharges (Q_{ref}, unit of mm h^{-1} multiplied by 5). Initial rainfall accumulation (PV_I, unit of mm multiplied by 1/2) is the accumulated rainfall volume during the 14 days prior to the flood rising limbs. Initial soil moisture (SM_I, %) is the average catchment soil moisture during the day prior to the flood rising limb. Flooding soil moisture (SM_F, %) is the average catchment soil moisture during the day of peak discharge. Soil moisture here denotes the upper 1-m soil moisture data simulated by the AWRA-L model at a daily resolution. Rainfall conditions contributing to floods are represented by rainfall volume (PV_F, unit of mm multiplied by 1/5) and rainfall duration (PD_F, h), which are obtained from the spatially nearest rainfall gauge for each catchment.

increase significantly as the percentage of catchment BA increases among different catchment groups (Figure S6 in Supporting Information S1). They are also comparatively stronger for small to median-sized floods in terms of peak discharges. Statistically, fire impacts on flood magnitudes significantly ($p < 0.01$) decrease as the peak discharge of reference undisturbed floods increases (Figure S7a in Supporting Information S1). Lower fire impacts can occur under larger volumes and longer durations of rainfall during floods, and the closer soil moisture is to saturation (Figures S7b-d in Supporting Information S1). For spatial scale effects, although smaller catchments did show larger basic flood magnitudes (mm h^{-1}) and larger absolute flood amplification, the relative changes of flood magnitudes seem unrelated to the catchment size (Figure S8 in Supporting Information S1), which may indicate that small-scale flood amplification can conduct to large spatial scales.

4. Discussion and Conclusion

Forest fires increase flood flows mainly by exacerbating the infiltration-excess runoff process. With the large loss of vegetation cover during the 2019–2020 forest fires (Qin et al., 2022), the decreased interception capacity (maximum interception volume) potentially reduces rainfall interception and increases throughfall during those flood events. More importantly, since the degree of vegetation changes during fires can be inherently related to the changes in soil hydraulic properties (Ebel et al., 2022), soil infiltration capacity (the rate of maximum infiltration) can be reduced below pre-fire values, resulting in critical rainfall-intensity thresholds controlling post-fire runoff (Liu et al., 2022; Nyman et al., 2014). Similar to the land use change effect (Rogger et al., 2017), such soil hydrophobicity can produce surface runoff when rainfall intensity exceeds infiltration capacity (Figure 4a), leading to higher flood risk in the first 2 years (Ebel, 2020).

Apart from the land surface changes, the divergent fire impacts in different rainfall regions are also linked with the generating mechanisms of flood events in 2020–2021. In the catchments with winter-dominated and uniform rainfall, floods may be mainly caused by infiltration-excess overland flow due to smaller rainfall accumulation and lower initial soil moisture before the floods (Figure 3). This type of process is usually very susceptible to reductions in the infiltration capacity (Blöschl, 2022) and can easily exacerbate small and medium floods after severe fires under high-intensity rainfall (Figure 4a). In most catchments with summer-dominated rainfall, soils

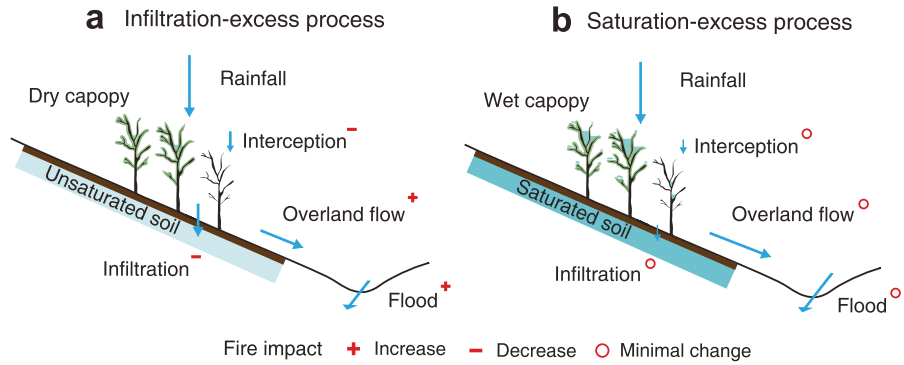

Figure 4. Explaining different forest fire impacts on flood magnitudes by different flood generating mechanisms. (a) Strong fire impact on river floods caused by intensified infiltration-excess overland flow, which is due to lower infiltration and interception. (b) Low fire impact on river floods under saturation-excess overland flow where soil moisture is close to saturation and the canopy is typically wet. Blue arrows are water fluxes (hydrological processes) and their lengths denote the relative rate. The red symbols in the top-right denote the fire impacts on these processes. Symbols "+," "–," and "o" represent a strong increase, a strong decrease, and a minimal change due to forest fire impacts, respectively.

are much closer to saturation at the beginning of major events in 2020–2021, so saturation-excess overland flow that is less susceptible to changes in the infiltration capacity (Blöschl, 2022) is more relevant (Figure 4b), which explains the lower relative changes in these regions. Given the regional divergence of flood responses, it is likely that, more generally, arid climates where infiltration excess processes dominate are more prone to forest fire effects on floods than humid climates with dominant saturation-excess overland flow.

While previous studies have demonstrated small-scale fire impacts, this study provides observational evidence that forest fire impacts on flood magnitudes can emerge across large geographic regions during the same period. The importance of land surface changes and dominant flood generating mechanisms were also highlighted in controlling post-fire flood amplification. While the implementation of the PCM here inevitably contains some uncertainty (such as the use of 20% as BA limit for defining burned and unburned catchments), the overall robust outcome of the PCM (Figure S9 in Supporting Information S1) indicates that it can benefit other statistical analysis of regional land surface changes. However, to advance our understanding, more specific efforts are further needed for disentangling processes, drivers, and scale effects of flood intensification underlying regional fire impacts.

The unprecedented scale of the 2019–2020 forest fires in southeast Australia may be an indication that climate change is already increasing the likelihood and magnitude of forest fires (Boer et al., 2020). As this study proves that mega forest fires can intensify flood magnitudes at a large scale, the hazards due to such floods may become more frequent in the future, especially for areas that experienced both intensifications of forest burned areas (Balch et al., 2022; Canadell et al., 2021; Coop et al., 2022) and short-duration rainfall extremes (Fowler et al., 2021; Westra et al., 2014) under anthropogenic climate change.

Conflict of Interest

The authors declare no conflicts of interest relevant to this study.

Data Availability Statement

All data used in this study are available from the websites as follows: continuous streamflow and precipitation data from BOM (http://www.bom.gov.au/waterdata/); SILO daily precipitation gridded data from the Queensland Department of Environment and Resource Management (https://www.longpaddock.qld.gov.au/silo/gridded-data/); the forest cover data and the land use data from the ABARES (https://www.agriculture.gov.au/abares/forestsaustralia/forest-data-maps-and-tools/spatial-data/forest-cover, https://www.agriculture.gov.au/abares/aclump/land-use/land-use-of-australia-2010-11_2015-16, respectively); the reservoir data from BOM (https://portal.wsapi.cloud.bom.gov.au/arcgis/apps/sites/#/australian-water-data-service/datasets/e8a0cd49c82a44ad-8f1d1660f8e7aa4e/data?geometry=-13.744%2C-52.209%2C-39.232%2C0.097); the seasonal rainfall zone data

from BOM (http://www.bom.gov.au/jsp/ncc/climate_averages/climate-classifications/index.jsp?maptype=-seasgrpb#maps); the 2019–2020 fire severity data from State agencies (Victoria, https://discover.data.vic.gov.au/dataset/fire-severity-map-of-the-major-fires-in-gippsland-and-north-east-victoria-in-2019-20-version-1-; New South Wales, https://datasets.seed.nsw.gov.au/dataset/fire-extent-and-severity-mapping-fesm-2019-20); the MODIS Collection 6 MCD64A1 BA data (https://lpdaac.usgs.gov/products/mcd64a1v006/); the root zone (top 1 m in the soil layer) relative soil moisture data simulated by AWRA-L from BOM (https://awo.bom.gov.au/products/historical/soilMoisture-rootZone/); an automatic outlet relocation algorithm from https://github.com/xiejx5/watershed_delineation; flow direction data from MERIT hydro (http://hydro.iis.u-tokyo.ac.jp/~yamadai/MERIT_Hydro/). A collection of the processed data can be accessed from Zenodo (https://doi.org/10.5281/zenodo.7571477).

Acknowledgments
The authors would like to thank the data support from the Australian BOM, the Australian Bureau of Agricultural and Resource Economics and Sciences (ABARES), and other researchers/agencies. Yongqiang Zhang acknowledges financial support from the National Key R&D Program of China (Grant 2022YFC3002804), the CAS Pioneer Talents Program, and the CAS-CSIRO drought propagation collaboration project. Günter Blöschl acknowledges the support from the Austrian Science Funds (Grant I 4776).

References

Abram, N. J., Henley, B. J., Sen Gupta, A., Lippmann, T. J. R., Clarke, H., Dowdy, A. J., et al. (2021). Connections of climate change and variability to large and extreme forest fires in southeast Australia. *Communications Earth & Environment*, *2*(1), 1–17. https://doi.org/10.1038/s43247-020-00065-8

Balch, J. K., Abatzoglou, J. T., Joseph, M. B., Koontz, M. J., Mahood, A. L., McGlinchy, J., et al. (2022). Warming weakens the night-time barrier to global fire. *Nature*, *602*(7897), 442–448. https://doi.org/10.1038/s41586-021-04325-1

Blöschl, G. (2022). Three hypotheses on changing river flood hazards. *Hydrology and Earth System Sciences*, *26*(19), 5015–5033. https://doi.org/10.5194/hess-26-5015-2022

Boer, M. M., Resco De Dios, V., & Bradstock, R. A. (2020). Unprecedented burn area of Australian mega forest fires. *Nature Climate Change*, *10*(3), 171–172. https://doi.org/10.1038/s41558-020-0716-1

Bowman, D. M. J. S., Kolden, C. A., Abatzoglou, J. T., Johnston, F. H., van der Werf, G. R., & Flannigan, M. (2020). Vegetation fires in the Anthropocene. *Nature Reviews Earth & Environment*, *1*(10), 500–515. https://doi.org/10.1038/s43017-020-0085-3

Bowman, D. M. J. S., Williamson, G. J., Gibson, R. K., Bradstock, R. A., & Keenan, R. J. (2021). The severity and extent of the Australia 2019–20 Eucalyptus forest fires are not the legacy of forest management. *Nature Ecology & Evolution*, *5*(7), 1003–1010. https://doi.org/10.1038/s41559-021-01464-6

Bren, L. J., & Lane, P. N. J. (2014). Optimal development of calibration equations for paired catchment projects. *Journal of Hydrology*, *519*, 720–731. https://doi.org/10.1016/j.jhydrol.2014.07.059

Brown, A. E., Zhang, L., McMahon, T. A., Western, A. W., & Vertessy, R. A. (2005). A review of paired catchment studies for determining changes in water yield resulting from alterations in vegetation. *Journal of Hydrology*, *310*(1–4), 28–61. https://doi.org/10.1016/j.jhydrol.2004.12.010

Cai, W., Borlace, S., Lengaigne, M., van Rensch, P., Collins, M., Vecchi, G., et al. (2014). Increasing frequency of extreme El Niño events due to greenhouse warming. *Nature Climate Change*, *4*(2), 111–116. https://doi.org/10.1038/nclimate2100

Cai, W., Wang, G., Santoso, A., McPhaden, M. J., Wu, L., Jin, F.-F., et al. (2015). Increased frequency of extreme La Niña events under greenhouse warming. *Nature Climate Change*, *5*(2), 132–137. https://doi.org/10.1038/nclimate2492

Canadell, J. G., Meyer, C. P., Cook, G. D., Dowdy, A., Briggs, P. R., Knauer, J., et al. (2021). Multi-decadal increase of forest burned area in Australia is linked to climate change. *Nature Communications*, *12*(1), 6921. https://doi.org/10.1038/s41467-021-27225-4

Chen, Y., Morton, D. C., Andela, N., van der Werf, G. R., Giglio, L., & Randerson, J. T. (2017). A pan-tropical cascade of fire driven by El Niño/Southern Oscillation. *Nature Climate Change*, *7*(12), 906–911. https://doi.org/10.1038/s41558-017-0014-8

Cheng, L., Zhang, L., & Brutsaert, W. (2016). Automated selection of pure base flows from regular daily streamflow data: Objective algorithm. *Journal of Hydrologic Engineering*, *21*(11), 06016008. https://doi.org/10.1061/(asce)he.1943-5584.0001427

Collar, N. M., Saxe, S., Rust, A. J., & Hogue, T. S. (2021). A CONUS-scale study of wildfire and evapotranspiration: Spatial and temporal response and controlling factors. *Journal of Hydrology*, *603*, 127162. https://doi.org/10.1016/j.jhydrol.2021.127162

Collins, L., Bradstock, R. A., Clarke, H., Clarke, M. F., Nolan, R. H., & Penman, T. D. (2021). The 2019/2020 mega-fires exposed Australian ecosystems to an unprecedented extent of high-severity fire. *Environmental Research Letters*, *16*(4), 044029. https://doi.org/10.1088/1748-9326/abeb9e

Collins, L., Griffioen, P., Newell, G., & Mellor, A. (2018). The utility of Random Forests for wildfire severity mapping. *Remote Sensing of Environment*, *216*, 374–384. https://doi.org/10.1016/j.rse.2018.07.005

Collischonn, W., & Fan, F. M. (2013). Defining parameters for Eckhardt's digital baseflow filter. *Hydrological Processes*, *27*(18), 2614–2622. https://doi.org/10.1002/hyp.9391

Coop, J. D., Parks, S. A., Stevens-Rumann, C. S., Ritter, S. M., Hoffman, C. M., & Varner, J. M. (2022). Extreme fire spread events and area burned under recent and future climate in the western USA. *Global Ecology and Biogeography*, *31*(10), 1949–1959. https://doi.org/10.1111/geb.13496

Ebel, B. A. (2020). Temporal evolution of measured and simulated infiltration following wildfire in the Colorado Front Range, USA: Shifting thresholds of runoff generation and hydrologic hazards. *Journal of Hydrology*, *585*, 124765. https://doi.org/10.1016/j.jhydrol.2020.124765

Ebel, B. A. (2022). The statistical power of post-fire soil-hydraulic property studies: Are we collecting sufficient infiltration measurements after wildland fires? *Journal of Hydrology*, *612*, 128019. https://doi.org/10.1016/j.jhydrol.2022.128019

Ebel, B. A., & Moody, J. A. (2017). Synthesis of soil-hydraulic properties and infiltration timescales in wildfire-affected soils. *Hydrological Processes*, *31*(2), 324–340. https://doi.org/10.1002/hyp.10998

Ebel, B. A., Moody, J. A., & Martin, D. A. (2022). Post-fire temporal trends in soil-physical and -hydraulic properties and simulated runoff generation: Insights from different burn severities in the 2013 Black Forest Fire, CO, USA. *Science of The Total Environment*, *802*, 149847. https://doi.org/10.1016/j.scitotenv.2021.149847

Eckhardt, K. (2005). How to construct recursive digital filters for baseflow separation. *Hydrological Processes*, *19*(2), 507–515. https://doi.org/10.1002/hyp.5675

Fowler, H. J., Lenderink, G., Prein, A. F., Westra, S., Allan, R. P., Ban, N., et al. (2021). Anthropogenic intensification of short-duration rainfall extremes. *Nature Reviews Earth & Environment*, *2*(2), 107–122. https://doi.org/10.1038/s43017-020-00128-6

Frost, A., & Shokri, A. (2021). *The Australian Landscape Water Balance Model (AWRA-L v7), Technical Description of the Australian Water Resources Assessment Landscape Model Version 7*. Bureau of Meteorology Technical Report.

Giglio, L., Boschetti, L., Roy, D. P., Humber, M. L., & Justice, C. O. (2018). The Collection 6 MODIS burned area mapping algorithm and product. *Remote Sensing of Environment*, *217*, 72–85. https://doi.org/10.1016/j.rse.2018.08.005

Godfree, R. C., Knerr, N., Encinas-Viso, F., Albrecht, D., Bush, D., Christine Cargill, D., et al. (2021). Implications of the 2019–2020 megafires for the biogeography and conservation of Australian vegetation. *Nature Communications*, *12*(1), 1023. https://doi.org/10.1038/s41467-021-21266-5

Hallema, D. W., Sun, G., Caldwell, P. V., Norman, S. P., Cohen, E. C., Liu, Y., et al. (2018). Burned forests impact water supplies. *Nature Communications*, *9*(1), 1–8. https://doi.org/10.1038/s41467-018-03735-6

Holgate, C. M., De Jeu, R. A. M., van Dijk, A. I. J. M., Liu, Y. Y., Renzullo, L. J., Vinodkumar, et al. (2016). Comparison of remotely sensed and modelled soil moisture data sets across Australia. *Remote Sensing of Environment*, *186*, 479–500. https://doi.org/10.1016/j.rse.2016.09.015

Jeffrey, S. J., Carter, J. O., Moodie, K. B., & Beswick, A. R. (2001). Using spatial interpolation to construct a comprehensive archive of Australian climate data. *Environmental Modelling & Software*, *16*(4), 309–330. https://doi.org/10.1016/S1364-8152(01)00008-1

Kean, J. W., Staley, D. M., & Cannon, S. H. (2011). In situ measurements of post-fire debris flows in southern California: Comparisons of the timing and magnitude of 24 debris-flow events with rainfall and soil moisture conditions. *Journal of Geophysical Research*, *116*(F4), F04019. https://doi.org/10.1029/2011jf002005

Kemter, M., Fischer, M., Luna, L. V., Schönfeldt, E., Vogel, J., Banerjee, A., et al. (2021). Cascading hazards in the Aftermath of Australia's 2019/2020 Black Summer wildfires. *Earth's Future*, *9*(3), e2020EF001884. https://doi.org/10.1029/2020ef001884

Khaledi, J., Lane, P. N. J., Nitschke, C., & Nyman, P. (2022). Wildfire contribution to streamflow variability across Australian temperate zone. *Journal of Hydrology*, *609*, 127728. https://doi.org/10.1016/j.jhydrol.2022.127728

King, A. D., Pitman, A. J., Henley, B. J., Ukkola, A. M., & Brown, J. R. (2020). The role of climate variability in Australian drought. *Nature Climate Change*, *10*(3), 177–179. https://doi.org/10.1038/s41558-020-0718-z

Lane, P. N. J., Sheridan, G. J., & Noske, P. J. (2006). Changes in sediment loads and discharge from small mountain catchments following wildfire in south eastern Australia. *Journal of Hydrology*, *331*(3–4), 495–510. https://doi.org/10.1016/j.jhydrol.2006.05.035

Larsen, I. J., Macdonald, L. H., Brown, E., Rough, D., Welsh, M. J., Pietraszek, J. H., et al. (2009). Causes of post-fire runoff and erosion: Water repellency, cover, or soil sealing? *Soil Science Society of America Journal*, *73*(4), 1393–1407. https://doi.org/10.2136/sssaj2007.0432

Letey, J. (2001). Causes and consequences of fire-induced soil water repellency. *Hydrological Processes*, *15*(15), 2867–2875. https://doi.org/10.1002/hyp.378

Liu, T., McGuire, L. A., Oakley, N., & Cannon, F. (2022). Temporal changes in rainfall intensity–duration thresholds for post-wildfire flash floods in southern California. *Natural Hazards and Earth System Sciences*, *22*(2), 361–376. https://doi.org/10.5194/nhess-22-361-2022

Loehman, R. A. (2020). Drivers of wildfire carbon emissions. *Nature Climate Change*, *10*(12), 1070–1071. https://doi.org/10.1038/s41558-020-00922-6

Moody, J. A., & Ebel, B. A. (2012). Hyper-dry conditions provide new insights into the cause of extreme floods after wildfire. *Catena*, *93*, 58–63. https://doi.org/10.1016/j.catena.2012.01.006

Moody, J. A., Shakesby, R. A., Robichaud, P. R., Cannon, S. H., & Martin, D. A. (2013). Current research issues related to post-wildfire runoff and erosion processes. *Earth-Science Reviews*, *122*, 10–37. https://doi.org/10.1016/j.earscirev.2013.03.004

Moritz, M. A., Batllori, E., Bradstock, R. A., Gill, A. M., Handmer, J., Hessburg, P. F., et al. (2014). Learning to coexist with wildfire. *Nature*, *515*(7525), 58–66. https://doi.org/10.1038/nature13946

Myneni, R., Knyazikhin, Y., & Park, T. (2015). MOD15A2H MODIS/Terra Leaf Area Index/FPAR 8-Day L4 Global 500 m SIN Grid V006 [Dataset]. NASA EOSDIS Land Processes DAAC. https://doi.org/10.5067/MODIS/MOD15A2H.006

Noske, P. J., Lane, P. N. J., Nyman, P., Van der Sant, R. E., & Sheridan, G. J. (2022). Predicting post-wildfire overland flow using remotely sensed indicators of forest productivity. *Hydrological Processes*, *36*(12). https://doi.org/10.1002/hyp.14769

Nyman, P., Sheridan, G. J., Smith, H. G., & Lane, P. N. J. (2014). Modeling the effects of surface storage, macropore flow and water repellency on infiltration after wildfire. *Journal of Hydrology*, *513*, 301–313. https://doi.org/10.1016/j.jhydrol.2014.02.044

Paul, M. J., LeDuc, S. D., Lassiter, M. G., Moorhead, L. C., Noyes, P. D., & Leibowitz, S. G. (2022). Wildfire induces changes in receiving waters: A review with considerations for water quality management. *Water Resources Research*, *58*(9), e2021WR030699. https://doi.org/10.1029/2021wr030699

Qin, Y., Xiao, X., Wigneron, J.-P., Ciais, P., Canadell, J. G., Brandt, M., et al. (2022). Large loss and rapid recovery of vegetation cover and aboveground biomass over forest areas in Australia during 2019–2020. *Remote Sensing of Environment*, *278*, 113087. https://doi.org/10.1016/j.rse.2022.113087

Rogger, M., Agnoletti, M., Alaoui, A., Bathurst, J. C., Bodner, G., Borga, M., et al. (2017). Land use change impacts on floods at the catchment scale: Challenges and opportunities for future research. *Water Resources Research*, *53*(7), 5209–5219. https://doi.org/10.1002/2017WR020723

Sikorska, A. E., Viviroli, D., & Seibert, J. (2015). Flood-type classification in mountainous catchments using crisp and fuzzy decision trees. *Water Resources Research*, *51*(10), 7959–7976. https://doi.org/10.1002/2015wr017326

Van Dijk, A. I. J. M., Beck, H. E., Crosbie, R. S., De Jeu, R. A. M., Liu, Y. Y., Podger, G. M., et al. (2013). The Millennium Drought in southeast Australia (2001–2009): Natural and human causes and implications for water resources, ecosystems, economy, and society. *Water Resources Research*, *49*(2), 1040–1057. https://doi.org/10.1002/wrcr.20123

Wang, G., & Cai, W. (2020). Two-year consecutive concurrences of positive Indian Ocean Dipole and Central Pacific El Niño preconditioned the 2019/2020 Australian "black summer" bushfires. *Geoscience Letters*, *7*(1), 1–9. https://doi.org/10.1186/s40562-020-00168-2

Ward, P. J., Jongman, B., Kummu, M., Dettinger, M. D., Sperna Weiland, F. C., & Winsemius, H. C. (2014). Strong influence of El Nino Southern Oscillation on flood risk around the world. *Proceedings of the National Academy of Sciences*, *111*(44), 15659–15664. https://doi.org/10.1073/pnas.1409822111

Wasko, C., Nathan, R., & Peel, M. C. (2020). Changes in antecedent soil moisture modulate flood seasonality in a changing climate. *Water Resources Research*, *56*(3), e2019WR026300. https://doi.org/10.1029/2019wr026300

Westra, S., Fowler, H. J., Evans, J. P., Alexander, L. V., Berg, P., Johnson, F., et al. (2014). Future changes to the intensity and frequency of short-duration extreme rainfall. *Reviews of Geophysics*, *52*(3), 522–555. https://doi.org/10.1002/2014rg000464

Williams, A. P., Livneh, B., McKinnon, K. A., Hansen, W. D., Mankin, J. S., Cook, B. I., et al. (2022). Growing impact of wildfire on western US water supply. *Proceedings of the National Academy of Sciences*, *119*(10), e2114069119. https://doi.org/10.1073/pnas.2114069119

Wine, M. L., Cadol, D., & Makhnin, O. (2018). In ecoregions across western USA streamflow increases during post-wildfire recovery. *Environmental Research Letters*, *13*(1), 014010. https://doi.org/10.1088/1748-9326/aa9c5a

Xie, J., Liu, X., Bai, P., & Liu, C. (2022). Rapid watershed delineation using an automatic outlet relocation algorithm. *Water Resources Research*, *58*(3), e2021WR031129. https://doi.org/10.1029/2021wr031129

Xu, Z., Zhang, Y., Zhang, X., Ma, N., Tian, J., Kong, D., & Post, D. (2022). Bushfire-induced water balance changes detected by a modified paired catchment method. *Water Resources Research*, *58*(11), e2021WR031013. https://doi.org/10.1029/2021wr031013

Yamazaki, D., Ikeshima, D., Sosa, J., Bates, P. D., Allen, G., & Pavelsky, T. (2019). MERIT hydro: A high-resolution global hydrography map based on latest topography datasets. *Water Resources Research*, *55*(6), 5053–5073. https://doi.org/10.1029/2019wr024873